



## Forged Steel Connecting Rod Design along with Analysis

Prathamesh S. Gorane<sup>1</sup>, Vijay B. Roundal<sup>2</sup>, Vijaykumar Javanjal<sup>3</sup>, Kuldeep A. Mahajan<sup>4</sup>

Sachin R. kandharkar<sup>5</sup>, Anil Shirgire<sup>6</sup>

<sup>1</sup> Associate Professor in Mechanical Engineering Department at Genba Sopanrao Moze College of Engineering, Balewadi, Pune, Maharashtra, India.

<sup>2</sup> Associate Professor in Mechanical Engineering Department at Genba Sopanrao Moze College of Engineering, Balewadi, Pune, Maharashtra, India.

<sup>3</sup> Associate. Professor, Department of Mechanical Engineering, DIT, Pimpri, Pune, India

<sup>4,5</sup> Assistant Professor, Department of Mechanical Engineering, M.E.S. College of Engineering, Pune-01

<sup>6</sup> Associate. Professor, Department of Civil Engineering, DIT, Pimpri, Pune, India

**Abstract:** The Connecting Rod is a critical part of an Internal Combustion Engine which undergo tensile, compressive and fatigue loading. It acts as an intermediate link or a part in between the piston that sustain gas force and crankshaft that converts into power. The piston pin exerts a push force whereas crank pin receives a pull force. This paper highlights the design and analysis along with different design methods and approach used for connecting rod by various researchers. Static analysis for tensile, compression and fatigue failure carried out on the forged steel connecting rod. Finally, results are discussed and factor of safety is determined for connecting rod.

**Keywords:** *Connecting Rod, Design, FEA analysis, Stress, Strain.*

### 1.0 Introduction

The connecting rod is central part between crankshaft as well as piston. Connecting rod is also responsible for converting reciprocating gesture of piston to rotary gesture of crank while transmitting push & pull from piston pin to crank pin.

Principle capacity of interfacing pole is to send push as well as pull from cylinder pin to wrench pin. As rule, it is auxiliary capacity is to pass on greasing up oil from base end to top & for example from wrench pin to cylinder pin & afterward for sprinkle of fly cooling of cylinder crown. Standard type of associating pole utilized in internal burning engine & cars appeared in Figure. 1.1



Figure 0.1: Schematic illustration of Connecting Rod

Researchers used different approaches to explore the connecting rod behavior through the analysis and experimental work. Baiyan He *et al.* [1], Presented; connecting rod, which used in diesel generator engine, along with its failure analysis. After approximately, 6000–10,000 hours of service; crack observed on toothed intersecting surface of connecting rod. Numerical analyses & material

characterization conducted on connecting rod to determine failure mechanism. Analysis of macro with microstructures; done by using optical microscope as well as microscope of scanning electron. Balasubramaniam *et.al.*[2], Revealed computational technique utilized in Mercedes-Benz utilizing instances of engine segments. As they would like to think, 2D FE models can utilize to acquire quick pattern explanations, & 3D FE models for more exact examination. The different individual burdens following up on interfacing bar utilized for performing reenactment & genuine pressure dissemination acquired by superposition. The heaps included idleness load, shooting load, press attack of bearing shell, & jolt powers. No conversations on enhancement or weakness, specifically, introduced. Banerji S. [3], Explored micro-alloyed forging used for heavy-duty diesel connecting rods. The different exercises that were important to conquer obstacles & make MA work for similar connecting rods summed up. Fashioned steel connecting rods utilized for majority requesting, large volume & larger pull diesel engine. Bhaskarjyoti Saikia *et al.* [4], Assessed fatigue & strength of diesel engine connecting rod to develop program made for power improvement with Turbo charging. During development & design of connecting rod, application of simulate design components has become an integral member. During design verification along with its validation, virtual recreation offers opportunities to lessen no of physical tests, which ultimately reduced development time & cost. Fatigue life, tensile & compressive stresses were considered during loading condition in simulation work of connecting rod. Bin Zheng *et al.*[5] , Analyzed fatigue life & stress distribution of connecting rod of light engine, vehicle engine using FEA & ANSYS software. Connecting rod is looked as vital part of engine, which is moving continuously. Initially connecting rod tends to fracture & ultimately to engine failure if reliability of component is not robust enough, fatigue failure of component may occur. It is only because of connecting rod fracture it tends to engine failure. C. Juarez *et al.* [6], Examined connecting bar utilized for age of electrical energy through diesel engine for its disappointment examination. A broad examination of connecting bar break zone just as material explored. Visual review, fractography, attractive molecule examination, synthetic examination, elastic & hardness testing, metallography, & microanalysis followed during trial examination. D. Gopinath *et al.*[7] explored weight reduction opportunities for connecting rod manufactured with aluminum, titanium & forged steel. Depending upon no of cylinders in engine, each vehicle has an IC engine needs minimum one connecting rod. In range of 108 to 109 cycles, connecting rod undergoes huge cyclic forces. These loads are because, of more tensile loads, because of inertia & because, of more compressive loads result of combustion. D. Taylor *et al.*[8] analyzed fatigue failure of an automotive crankshaft, which results under loading test condition in torsion & bending. From stress concentrations failures occurs whose area differed with stacking type. An identical K strategy, which; known as ‘break modeling’, utilized, in request to portray seriousness of pressure fixation. From static-load, limited component (FE) investigation to discover successful pressure power (K) values this method used for modeling approach. For material failure, it expected to occur if this was more than threshold  $K_{th}$  & subsequently cyclic K value can found. Dan Yang *et al.* [9] examined factually & decided powerless situation of connecting bar. During engine activity, connecting rods exposed to complex burden. The FEA model was set up once heap & limit states of connecting pole found by engine & kinematics examination. To anticipate exhaustion life of connecting bar under consistent plentiful-ness stacking & cyclic stacking of two distinct burdens weariness life & wellbeing variables of connecting bar are broke down this will give successful direction to plan of connecting bar. Dilip Verma *et al.* [10] carried out, FEA for two different materials. Connecting rod is highly critical & re-searchable one in sequence of components of

automobile engine. Connecting rod is middle link between crank & piston. Usually connecting rods produced with material as carbon steel. However, in current scenario aluminium alloys are getting its application in connecting rod.

## 2.0 Materials and Method

The present study of static analysis of original design for connecting rod used in Discover 100cc bike.

The connecting rod design involves of I cross-section at shank portion [11]. Input considerations defined as mentioned below. The present mass of connecting rod is 0.099 kg. The calculations for present design are as followed.

Input parameters for design calculations of Original Discover Connecting Rod

Bore diameter	D	= 47 mm
Crank radius	R	= 27.2 mm
Crank speed	N	= 2000 RPM
Firing angle	$\theta$	= 90 - 110
Length of connecting rod	L	= 92 mm
Maximum gas pressure	P <sub>max</sub>	= 2 MPa.
Weight of reciprocating masses	Mr	= 0.474 Kg

Specifications of Forged Steel Material

First Material		= Forged Steel
Forged Steel Density		= 8.031 g/cm <sup>3</sup>
Forged Steel Coefficient of Thermal Expansion		= 12.0 $\mu$ m/m · K
Forged Steel Specific Heat		= 4.340 kJ/kg
Forged Steel Thermal Conductivity		= 60.50 (w/mK)
Forged Steel Resistivity		= 1.70 $\Omega$ .cm
Forged Steel Compressive Yield Strength		= 625.00 (MPa)
Forged Steel T. Yield Strength		= 625.0 (MPa)
Forged Steel T. Ultimate Strength		= 827.0 (MPa)
Forged Steel Compressive Ultimate Strength		= 827.00 (MPa)
Forged Steel Poisson's ratio	$\mu$	= 0.280
Forged Steel Young's Modulus	E	= 210.0 GPa

A solid model of the connecting rod as observed in diagram was generated using appropriate modeling software package Catia V5 modeler. From figure 1.2, it can be seen that connecting rod is symmetric about axis line joining centres of gudgeon pin & crank end. Therefore connecting rod has modeled as symmetric model with the help of suitable modeling software i.e. Catia V5 modeler. The volume of connecting rod is 11873.2 mm<sup>3</sup> whereas mass of connecting rod is 0.099 kg.

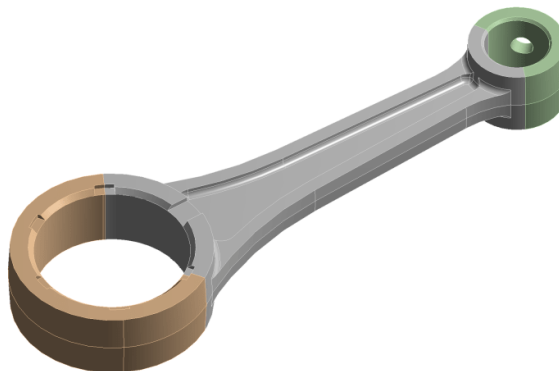


Figure 1.2: Geometry of Original Discover Connecting Rod

The figure 1.3 shows meshed model of connecting rod prior to optimization. Finite Element Analysis was done in Ansys 19 software. Finite element mesh was generated using hexahedral elements with maximum face size as 1.5 mm & number of elements are 15920 with 55405 number of nodes. Coarse meshing performed for reducing computational time. Purpose of selecting hexahedral element was to have better accuracy & better result for fatigue life estimation. According to four load cases, the boundary condition were applied [12-16].

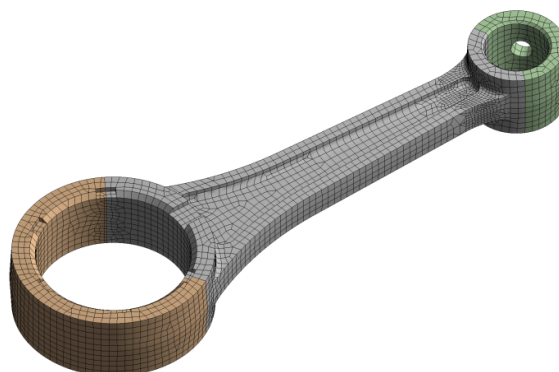


Figure 1.3 : Meshed Geometry of Original Discover Connecting Rod

Grid sensitivity analysis performed for the selection of the optimum element size. The element size was selected as mentioned above from the graph obtained from the grid sensitivity analysis. From the analysis it can be seen that at element size 1.1 & 1.5 the stress as well as deformation as closer to each other. Hence it will be good if there values are considered for the meshing purpose. But to reduce the computation time and to get better results, cell size is considered as 1.5mm.

## 2.1 Force Calculation for Design of Connecting Rod

### 2.1.1 Force due to Combustion Pressure:

We have equation as [12],

$$F_g = \text{Utmost Pressure of the Gas} \times \text{Piston Area}$$

$$F_g = P_{\max} \times \frac{\pi D^2}{4}$$

Where,  $P_{\max} = 2\text{MPa}$

$$P_{\max} = 2 \times 10^6 \text{ N/m}^2$$

Hence,

$$F_g = 2 \times 10^6 \times \frac{\pi \times 0.047^2}{4}$$

$$F_g = 3469.9 \text{ N}$$

$$F_g = 3.4699 \text{ KN}$$

The maximum gas pressure because of combustion is 3.4699 KN.

**2.1.2 Force due to Inertia of Reciprocating Masses:**

$$F_i = 0.474 \times \left( \frac{2 \times \pi \times 2000}{60} \right)^2 \times 0.027 \times \left( \cos 10 + \frac{\cos(2 \times 10)}{3.3823} \right)$$

$$F_i = 0.474 \times 43864.9 \times 0.027 \times 1.2626$$

$$F_i = 708.8021 \text{ N}$$

The Load cases applied for proposed case study are shown in the figure 1.4 and nature of load mentioned in the table 1.1. After applying boundary conditions the problem is solved in Ansys.

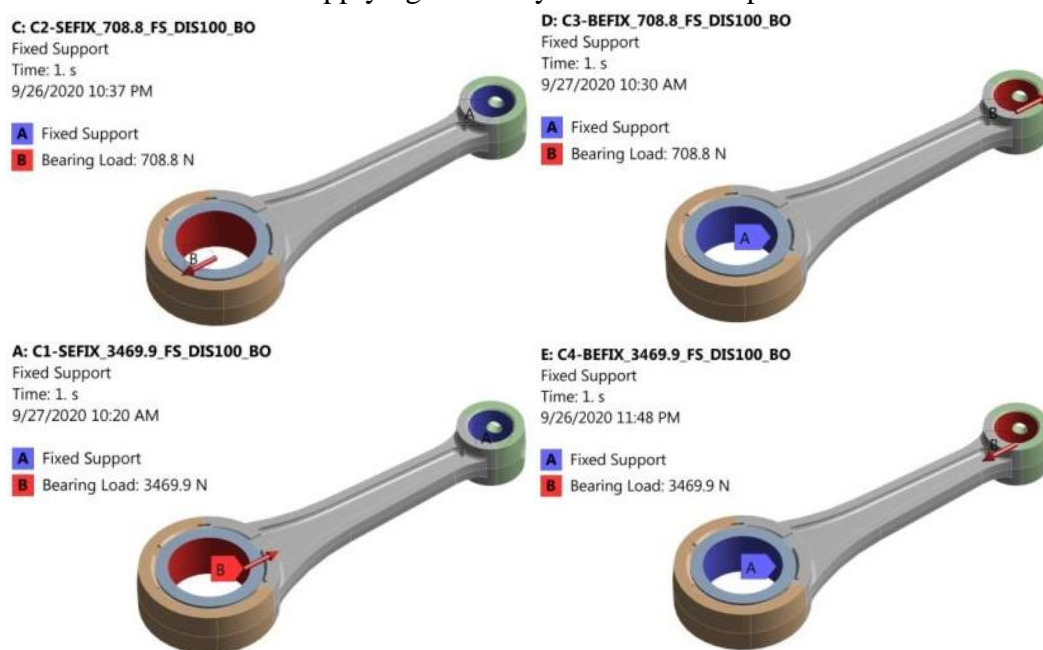


Figure 1.4: Load Cases applied for case study of Discover connecting rod

	Crank end (big end)			piston end (small end)		
Load Case	Nature of Load	Boundary Conditions	Magnitude	Nature of Load	Boundary Conditions	Magnitude
1	tensile Loading	Load applied on inner circumference	708.8 N	Nil	constrained	Nil
2	Nil	constrained	Nil	tensile Loading	Load applied on inner circumference	708.8 N
3	compressive Loading	Load applied on inner	3469.9 N	Nil	constrained	Nil

		circumference				
4	Nil	constrained	Nil	compressive Loading	Load applied on inner circumference	3469.9 N

Table 1.1: Load cases applied for proposed case study

### 3.0 Result and discussion

The static analysis carried out on the connecting rod and the total deformation plots are as shown in Figure 1.5. During tensile force is applied at crank end, section of maximum and minimum total deformation can be observed from total deformation. When tensile effort of magnitude 708.8 N is applied at crank end & piston end was inhibited, then location of maximum total deformation can be noted as 0.0071509 mm, while minimum total deformation was noted as 0.0 for forged steel.

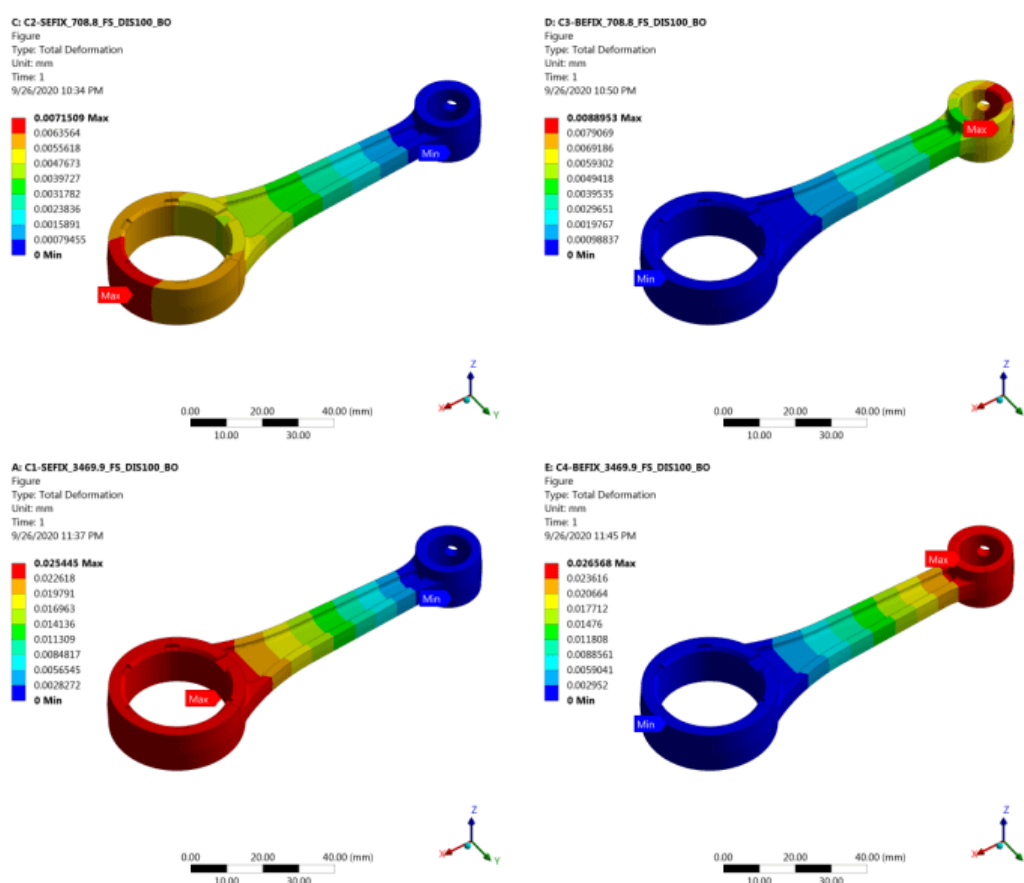


Figure 1.5: Total Deformation Diagram for Forged Steel Material

The location of maximum total deformation is located in the region near crank end, while minimum total deformation is located in the section away from crank end. While stretchable pressure applied at piston end, top as well as bottom most total deformation, noticed from total deformation as shown in figure 1.5 of forged steel. When stretchable exertion of magnitude 708.8 N applied at piston end as well as crank end reserved, and then the region of topmost total deformation noted as 0.0088953 mm.

As magnitude of 3469.9 N compression forces deployed the section of maximal total deformation noted as 0.0254450 mm.

At the time of compressive exertion is applied at small end, the region of highest as well as lowest total deformation can be seen from total deformation outline as shown in figure of forged steel. Locality of highest total deformation noted as 0.0265680 mm.

The equivalent stress observed on the connecting rod shown in Figure 1.6. At time of tensile force is applied at crank end, the region of maximum and minimum equivalent stress can be seen from equivalent stress diagram as shown in figure 1.6 of forged steel. When tensile pressure of magnitude 708.80 N deployed at crank as well as piston end guarded, and then notes location of maximum equivalent stress, as 27.361 MPa, while minimum equivalent stress noted as 0.00129050 MPa for forged steel.

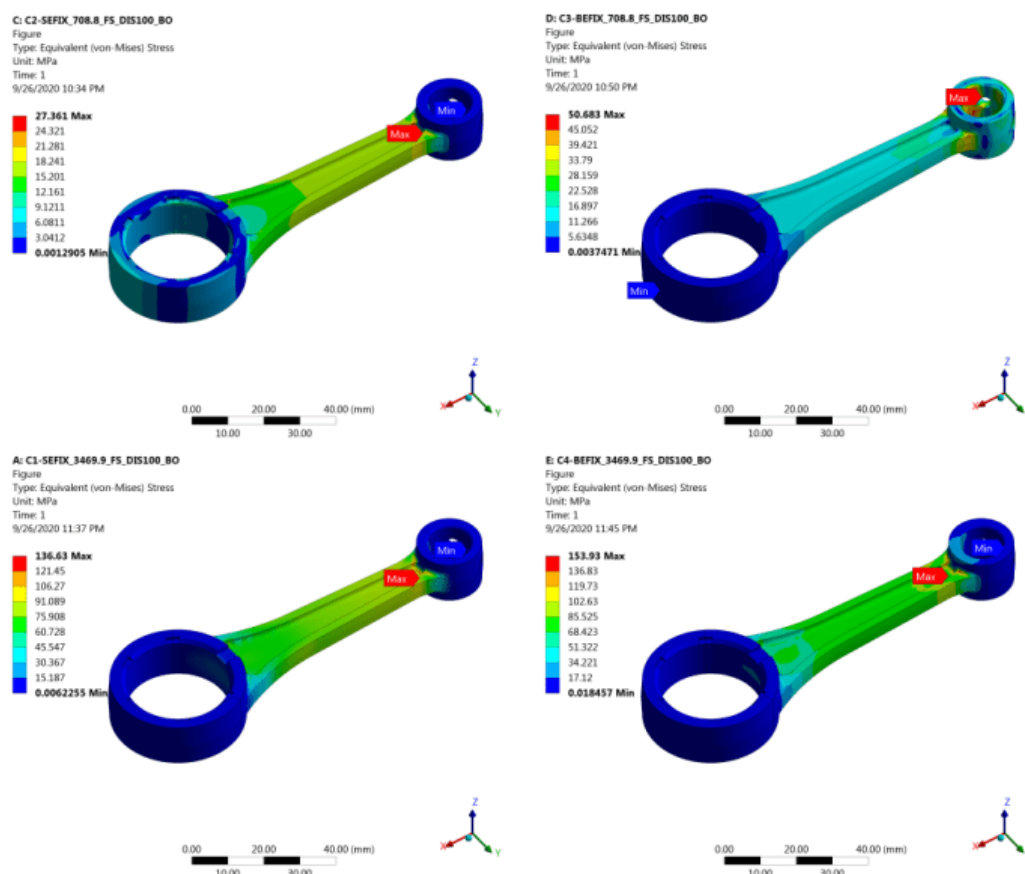


Figure 1.6: equivalent stress for Forged Steel Material

During stretchable pressure applied at piston end, section of top most as well as bottom, most equivalent stress observed from equivalent stress as shown in figure 1.6 of forged steel. When stretchable effort of magnitude 708.80 N applied at piston end & crank end inhibited, the region of top most equivalent stress noted as 50.683 MPa, while bottom most equivalent stress noted as 0.00374710 MPa for forged steel. The region of top most equivalent stress observed in the portion away from crank end, while bottom most equivalent stress observed in the portion near crank end. Section of maximal equivalent stress noted as 136.630 MPa, while minimal equivalent stress noted as 0.00622550 MPa for forged steel.

When compressive loading applied at small end, then location of highest as well as lowest equivalent stress identified from equivalent stress outline as shown in figure 1.6 of forged steel.



compressive force of magnitude 3469.90 N applied at small end and the big end was constrained, locality of highest equivalent stress noted as 153.930 MPa, while lowest equivalent stress noted as 0.01845700 MPa for forged steel.

The connecting rod is undergoing fatigue loading during the operative condition. This encourages to understand the fatigue life of the connecting rod. In this context fatigue life plots are as shown in the Figure 1.7.

**Static inspection – finding of fatigue life for discover connecting rod, for forged steel material.**

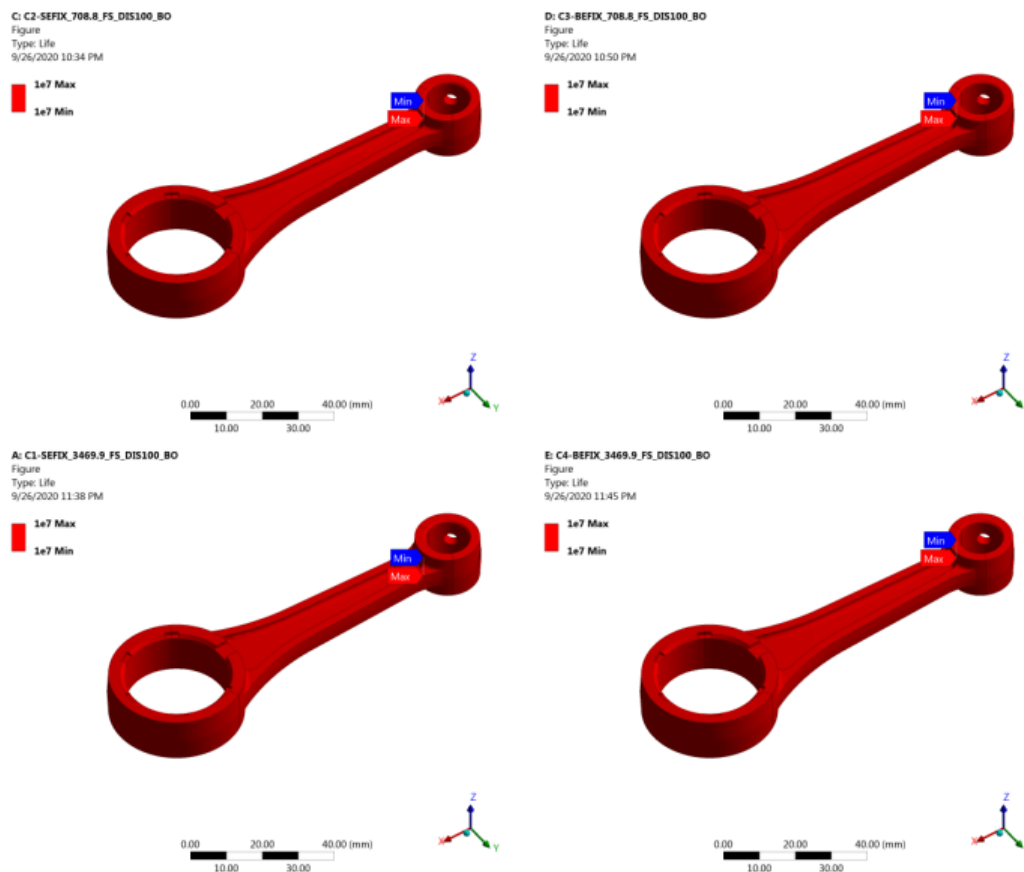


Figure 1.7: Fatigue Life Diagram for Forged Steel Material

It has been noticed that, while tensile force applied at crank end, locality of maximum and minimum fatigue life noticed from fatigue life sketch as shown in figure 1.7 of forged steel. Location of maximum fatigue life; seen in locality near piston end, while minimum fatigue life noticed, in section away from crank end. When stretchable pressure applied at piston end, then location of top most as well as bottom most fatigue life identified from fatigue life outline as shown in figure of forged steel.

At time of compression, effort applied at big end, the region of maximal and minimal fatigue life seen from fatigue life diagram as shown in figure 1.7 of forged steel. When compression exertion of magnitude 3469.889 N deployed at big as well as small end guarded, and then section of maximal fatigue life noted as 1.0 E+07 cycles, while minimum fatigue life noted as 1.00 E+07 cycles for forged steel. During compressive exertion is applied at small end, section of highest as well as lowest fatigue life can be observed from fatigue life figure as shown in figure 1.7 of forged steel.



compressive force of magnitude 3469.889 N applied at small end & big end inhibited, then locality of highest fatigue, life noted as 1.0 E+07 cycles, while bottom most fatigue life noted as 1.00 E+07 cycles for forged steel. Locality of highest fatigue life; identified in the section near small end, while lowest fatigue life observed in the region away from big end.

Based on the results obtained from deformation, stress and fatigue life of the connecting, the factor of safety becomes important parameter for the connecting rod analysis. The factor of safety also analysed at both end of the connecting rod by applying the tensile and compressive loads. The results of the analysis of factor of safety are as shown in Figure 1.8.

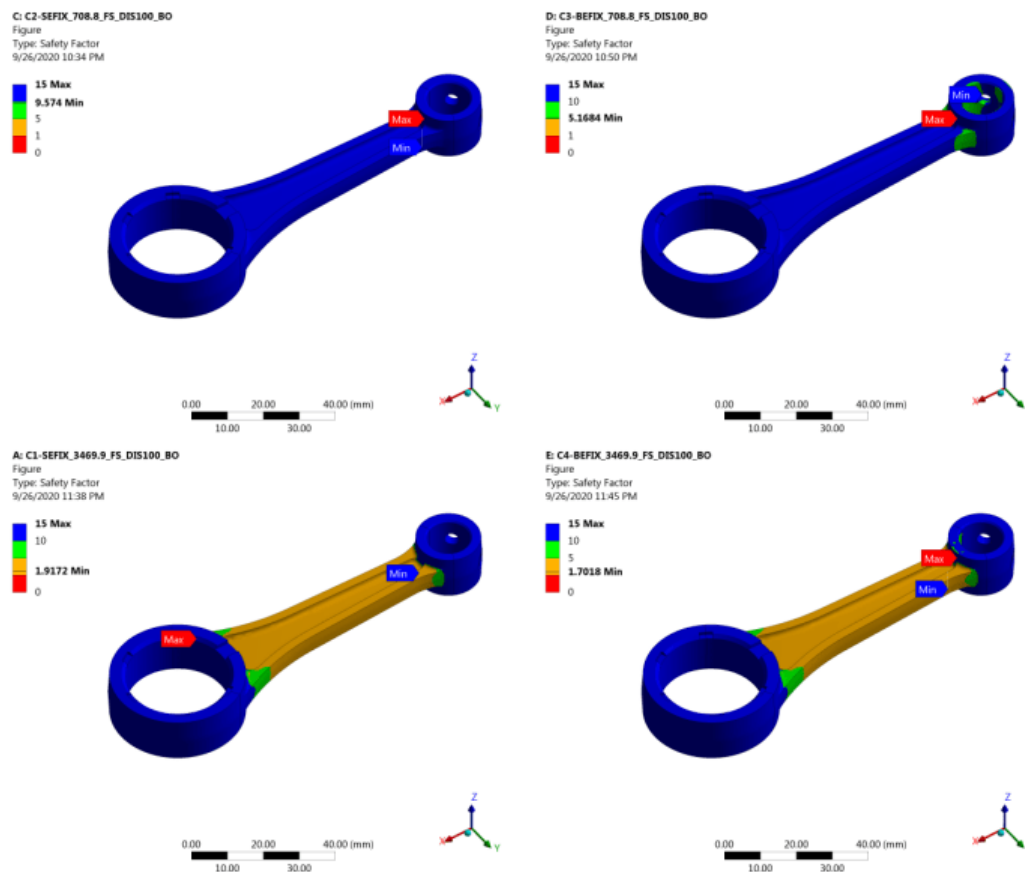


Figure 1.8: Safety Factor Diagram for Forged Steel Material

At time of tensile pressure is applied at crank end, the region of highest as well as lowest safety factor can be seen from safety factor sketch as shown in figure 1.8 of forged steel. When tensile exertion of magnitude 708.8021 N is deployed at crank as well as piston end was reserved, then location of maximum safety factor can be noted as 15.0, while minimal safety factor was noted as 9.5740 for forged steel. Topmost safety factor noted as 15.0, whereas lowest safety factor noted as 5.1684 for forged steel during the analysis.

While compression exertion applied at big end, locality of top most as well as bottom most safety factor noticed from safety factor diagram as shown in figure of forged steel. When compression pressure of magnitude 3469.8890 N is applied at big end as well as small end was guarded, then section of maximal safety factor can be noted as 15.0, while minimum safety factor was noted as 1.9172 for forged steel.

When compressive effort applied at small end, then location of maximal and minimal safety factor identified from safety factor figure as shown in figure of forged steel. When compressive effort of

magnitude 3469.8890 N applied at small end and the big end inhibited, and then locality of highest safety factor can be noted as 15.0, while bottom most safety factor was noted as 1.7018 for forged steel.

From the above study the result is discussed summarized in the table 1.2 below.

Table 1.2: Static Analysis Result for Connecting Rod for Forged Steel Material

Connecting Rod used in Discover								
Case	Deformation in mm		equivalent stress in MPa		Fatigue Life in Cycles		Safety Factor	
	Minimum	Maximum	Minimum	Maximum	Minimum	Maximum	Minimum	Maximum
1	0.0	0.0071509	0.0012905	27.361	$1 \times 10^{07}$	$1 \times 10^{07}$	9.574	15
2	0.0	0.0088953	0.0037471	50.683	$1 \times 10^{07}$	$1 \times 10^{07}$	5.1684	15
3	0.0	0.0254450	0.0062255	136.630	$1 \times 10^{07}$	$1 \times 10^{07}$	1.9172	15
4	0.0	0.0265680	0.0184570	153.930	$1 \times 10^{07}$	$1 \times 10^{07}$	1.7018	15

#### 4. Conclusions

During study, literature review of numerous aspects of connecting rods in various load condition & stress investigation, performed & discussed. In order to get exact or better methodology for development of connecting rod for its design, analysis & optimization study done on several aspects of connecting rod.

Then forged steel material was selected for assessments of connecting rod parameters of connecting rod. I cross sections selected for assessments of connecting rod parameters. Once results of selected cases obtained then best suitable material & cross section considered for topology optimization. Topology optimization performed in order to go for weight optimization. The results achieved from topology optimization as well as FEA, used in process of geometry optimization. As soon as geometry was optimized, the different 4 load cases were exerted and results were attended. These attended outcomes or results matched with present connecting rod & concluding remark made.

#### REFERENCES

- [01] Mr. Bai-yan He, Mr. Guang-da Shi, Mr. Ji-bing Sun, Mr. Si-zhuan Chen and Mr. Rui Nie (2013), Crack analysis on the toothed mating surfaces of a diesel engine connecting rod, Elsevier - Engineering Failure Analysis, Volume No. 13, Issue No. 7, Page No. 79-89
- [02] Mr. Balasubramaniam B., Mr. Svoboda M. and Mr. Bauer W. (1991), Structural optimization of I.C. engines subjected to mechanical and thermal loads, Computer Methods in Applied Mechanics and Engineering, Volume No. 89, Issue No. 3, Page No. 337-360
- [03] Mr. Banerji S. K., (1996), Application of microalloyed forgings for heavy-duty diesel-engine connecting rods and other components, Mineral, Metals and Materials Society, Volume No. 12, Issue No. 2, Page No. 375-389
- [04] Mr. Bhaskarjyoti Saikia, Mr. Piyush Ranjan, Mr. Remesan Chirakkal and Mr. Vasundhara V. Arde (2015), Establishment Of Methodology For Prediction Of Fatigue Life Of Connecting Rod Through Virtual Simulation, SAE International, Volume No. 10, Issue No. 1, Page No. 47-51
- [05] Mr. Bin Zheng, Mr. Yongqi Liu and Mr. Ruixiang Liu (2013), Stress And Fatigue Of

- Connecting Rod In Light Vehicle Engine, The Open Mechanical Engineering Journal, Volume No. 7, Issue No. 8, Page No. 14-17
- [06] Mr. C. Juarez, Mr. F. Rumiche, Mr. A. Rozas, Mr. J. Cuisano and Mr. P. Lean (2016), Failure Analysis Of A Diesel Generator Connecting Rod, Elsevier - Case Studies in Engineering Failure Analysis, Volume No. 10, Issue No. 1, Page No. 48-51
- [07] Mr. D. Gopinath and Mr. Ch. V. Sushma (2015), Design And Optimization Of Four Wheeler Connecting Rod Using Finite Element Analysis, Elsevier - Science Direct - Materials Today, Volume No. 12, Issue No. 8, Page No. 2291-2299
- [08] Mr. D. Taylor A., Mr. W. Zhou B., Mr. A. J. Ciepalowicz B. and Mr. J. Devlukia (1998), Mixed-Mode Fatigue From Stress Concentrations: An Approach Based On Equivalent Stress Intensity, Elsevier - International Journal of Fatigue, Volume No. 11, Issue No. 9, Page No. 15-21
- [09] Mr. Dan Yang, Mr. Zhen Yu, Mr. Wentao Cheng and Mr. Leilei Zhang (2017), Fatigue Analysis of Engine Connecting Rod Based on Workbench, 7th International Conference on Mechatronics, Computer and Education Informationization, Volume No. 10, Issue No. 1, Page No. 47-51
- [10] Mr. Dilip Verma, Mr. Mohit Juneja, Mr. Shubham Jain, Mr. Vinayak Rathore, Mr. Wahid Khan and Mr. Harshit Goyal (2016), Design and Optimization of Connecting Rod, International Journal of Mechanical and Industrial Technology, Volume No. 4, Issue No. 1, Page No. 38-43
- [11] Mr. Prathamesh S. Gorane and Dr. Kashinath H. Munde, Analysis and Optimization of a Connecting Rod (2020), IJSRD - International Journal for Scientific Research & Development, Vol. 8, Issue 9, 2020, ISSN (online): 2321-0613
- [12] Mr. Prathamesh S. Gorane and Dr. Kashinath H. Munde, Finite Element Analysis of Optimized Connecting Rod (2020), IJSRD - International Journal for Scientific Research & Development, Vol. 8, Issue 9, 2020, ISSN (online): 2321-0613
- [13] Dr. Prathamesh S. Gorane and Dr. Vijay B. Roundal, Connecting Rod Design along with Analysis a Review (2022), Journal of Automation and Automobile Engineering, e-ISSN: 2582-3159, Volume-7, Issue-1 (January-April, 2022).
- [14] Roundal Vijay Baburao and Dr. Kashinath H. Munde, Dynamic Formulation of Stiffness Matrix for Free Vibration Analysis (2020), IJSRD, ISSN (online): 2321-0613, Volume-8, Issue-9 (Nov, 2020)
- [15] Roundal Vijay Baburao and Dr. Kashinath H. Munde, Methodology for Dynamic Stiffness Matrix Formulation for Free Vibration Analysis (2020), IJSRD, ISSN (online): 2321-0613, Volume-8, Issue-9 (Nov, 2020)
- [16] Dr. Vijay B. Roundal & Dr. Prathamesh S. Gorane, Free vibration analysis for Dynamic Stiffness formulation- Literature review (2022), Journal of Mechanical and Mechanics Engineering, e-ISSN: 2581-3722, Volume-8, Issue-1 (January-April, 2022)